

# BUCKLING ANALYSIS OF NON-RECTANGULAR STIFFENED SHELL STRUCTURES

A. Kiehne, P. Horst

Institute of Aircraft Design and Lightweight Structures, TU Braunschweig  
Hermann-Blenk-Straße 35, 38108 Braunschweig  
Germany

## ABSTRACT

Usually, fuselage structures are stiffened by longitudinal and circumferential structural elements in a way that rectangular fields evolve. In the case of modern manufacturing technologies for aircraft structures, new topologies can be produced and possibly replace a conventional fuselage design. This paper deals with the buckling analysis of metallic non-rectangular stiffened structures with triangular skin panels. In order to assess the benefits, the buckling behaviour of triangular and rectangular stiffened structures due to various load combinations is compared.

## NOTATION

$a$	length of skin panel, plate or shell
$A$	ultimate strain
$A_{fr}$	cross sectional area of the frame
$A_{str}$	cross sectional area of the stringer
$A_{til,2}$	cross sectional area of the tilted stiffeners of second triangular structure
$A_{tri,1}$	cross sectional area of the stiffening members of first triangular structure
$b$	width of skin panel, plate or shell
$E$	modulus of elasticity
$F_C$	applied compression force
$F_{C, cr}$	compressive critical buckling load
$F_S$	applied shear force
$F_{S, cr}$	shear critical buckling load
$k$	buckling factor
$\ell_{fr}$	frame length in the considered skin panel
$\ell_{str}$	stringer length in the considered skin panel
$\ell_{til}$	tilted stiffener length in the considered skin panel
$m$	number of buckling half cycles
$r$	shell radius
$R_m$	tensile strength
$R_{p0,2}$	proportional limit
$t$	thickness of skin panel, plate or shell
$V_{sum}$	stiffening member volume for one skin panel
$\alpha$	panel aspect ratio
$\varepsilon$	strain
$\varepsilon_W$	real strain
$\lambda$	load factor for buckling
$\nu$	Poisson's ratio
$\sigma$	stress
$\sigma_{cr}$	compressive critical buckling stress
$\sigma_W$	real stress
$\omega$	factor for shell curvature

## 1. INTRODUCTION

The fuselage of an aircraft is a stiffened shell structure. In the conventional fuselage design stringers in longitudinal direction and frames in circumferential direction are utilized to stiffen the thin skin. In most cases the stiffening members are riveted to the skin.

Buckling due to compression, shear or a combination of both are the typical load types for fuselage structures.

New developments, like Highspeed Cutting enable manufacturers to produce integral stiffened metallic aircraft structures of nearly arbitrary topology.

Integral stiffening concepts like non-rectangular stiffened structures possibly have advantages in terms of buckling behaviour, when compared to a conventional stringer-frame fuselage structure. In addition, integral stiffening concepts have a great weight reduction potential, which subsequently means saving costs.

Comparative numerical analyses were carried out with the finite element solver ANSYS to show the potentials of integral stiffening concepts. During the analyses the buckling behaviour of an integral non-rectangular stiffened structure and a conventional stiffened structure were compared. The numerical results are compared to analytical solutions. The problem is, that there are only a few analytical approaches which describe the buckling behaviour due to compression, shear or combined load of non-rectangular stiffened structures.

First, a reference structure with conventional stiffener assembly was defined. Then, two different non-rectangular stiffened structures with triangular skin panels were designed based on the reference structure. These triangular structures have the same volume as the reference structure, i.e. the same weight. During the analyses, the advantages of the non-rectangular stiffened structures are quantified.

## 2. GENERIC REFERENCE STRUCTURE

A fuselage panel stiffened with stringers and frames, from the section behind the wing is defined as a reference structure. The geometry, finite element model and boundary conditions of the stiffened panel are described below.

The numerical results for the reference structure are compared to analytical solutions. For rectangular stiffened plates and shells generic various analytical approaches exist, which are consulted for comparison.

### 2.1. Geometry

As shown in FIG 1, the rectangular stiffened reference structure comprises one skin panel with a half skin panel

on each side. The aspect ratio of the considered skin panel is equal to the aspect ratio of the lower side shell and the lower shell skin panels of a commercial aircraft with two aisles. These are the regions of the fuselage affected mainly by buckling stress.

### 2.1.1. Stiffening members

The reference panel is stiffened by longitudinal stringers and circumferential frames and clips. The stringers and frames have a thin walled Z-cross section. The frames are joined to the skin by clips with a L-cross section. See FIG 1 for the spacing of frame and stringer.

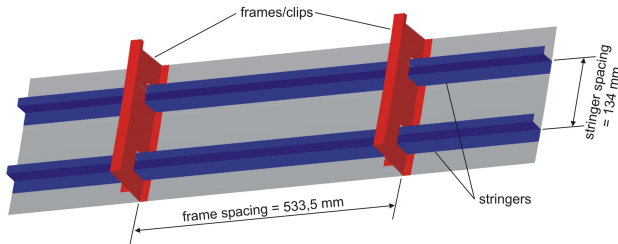


FIG 1. Geometry of the generic reference panel

## 2.2. Finite element model

The finite element model is generated in ANSYS. The mesh density, used element types, boundary conditions and assumptions for the finite element are described in detail below.

### 2.2.1. Assumptions for the finite element model

Assumptions are made in order to reduce the complexity of modelling. A highly detailed finite element model is comprised of many degrees of freedom. This means consequently a lengthy calculation time.

The three-dimensional fuselage panel is modelled by two-dimensional thin shell element for the skin and all stiffening members. A finite element model with three-dimensional continuum elements is not necessary because the elements have thin thicknesses and the material is homogeneous.

Normally fuselage skin panels do not have a uniform skin thickness. There are regions with pocketing and doubler regions, for instance fail-safe straps and waffle doublers under the frames and stringers. In this paper the buckling behaviour of an integral non-rectangular stiffened structure and a conventional rectangular stiffened structure are compared. Hence, the finite element model takes such complexity into account.

The skin elements have a constant thickness of 2 mm. The thickness of the stringer or clip flange is added to the skin thickness in the stiffening range. This combination of stiffener and skin is modelled by one shell element. In practice, a continuous connection like bonding or welding is assumed between the skin and the stiffener. Otherwise the finite element model cannot detect effects like inter-rivet buckling. The influence of several joints like bonding, riveting or welding is not of interest in this investigation.

In reference to the above-mentioned finite element modelling considerations, preferably the connection between the longitudinal stringers and the circumferential frames should be simplified. However, the clips between

the stringers and frames keep the upper region of the frames attached and therefore should not be disregarded. Instead of the clips the connection between stringers and frames is modelled by a longitudinal spring element with a high stiffness. Moreover, the springs elevate the restraining level for the longitudinal stringers. In ANSYS a three-dimensional spring element is the COMBIN14-element with three degrees of freedom (translations in the nodal x, y, and z directions) at each node [6].

In his work Heitmann [7] uses similar assumptions and shows that the results of the numerical analyses correspond to the results of tests.

### 2.2.2. Mesh density and element types

The skin and the stiffeners implemented using shell elements; thereby the central surface of the shell element is the reference surface. The 4-node element SHELL181 with six degrees of freedom at each node (translations in the x, y, and z directions, and rotations about the x, y, and z-axes) is chosen in ANSYS. SHELL181 is suited for linear and large strain nonlinear applications [6]. The element provides bending and membrane stiffness.

Simply supported rectangular plates uniformly compressed in one direction are modelled with various element types and mesh densities. Two element types with linear shape functions (3-node element and 4-node element) and two element types with quadratic shape functions (6-node element and 8-node element) are used for the finite element model. Within a linear buckling analysis in ANSYS the five lowest eigenvalues are calculated for all discretisations. The numerical results and the analytical solution of the differential equation (1) are compared. With regard to the number of degrees of freedom, the 4-node elements show the best convergence behaviour. However, fine meshes should be used to allow for critical mode shapes with a high number of half cycles of buckling.

### 2.2.3. Boundary conditions

The modelled panel is a section of a whole cylindrical fuselage. The boundary conditions of the panel are suited to the real boundary conditions in the fuselage. The fuselage panel receives periodical boundary conditions. FIG 2 shows the finite element model with the numbering of the boundaries and applied forces.

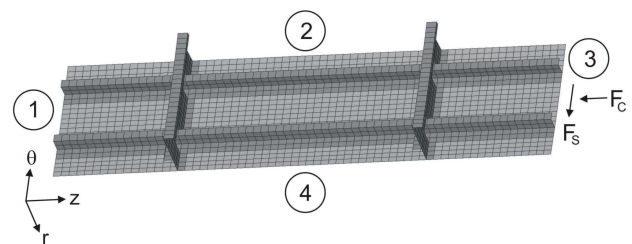


FIG 2. Finite element model with applied forces

Each node on the circumferential boundary 2 is connected by a Multi Point Constraint (MPC) for each degree of freedom with the corresponding node on boundary 4, with the same r and z coordinate. A MPC means that a displacement boundary condition of a node is expressed by the condition of at least one other node. The radial displacements  $U_r$  and rotations about the r,  $\theta$  and z-axes of the corresponding nodes on boundaries 1 and 3, with

the same  $r$  and  $\theta$  coordinate, are connected by MPC's in order to simulate periodic boundary conditions.

The force application occurs on the longitudinal boundaries 1 and 3. Compression is applied on all nodes of the skin and stiffeners, whereas the shear is only applied on the skin nodes. All skin and stiffener nodes on boundary 1 are fixed in longitudinal direction  $U_z$  and only the skin nodes are additionally fixed in circumferential direction  $U_\theta$ . The load is applied to one skin node on boundary 3. The circumferential and longitudinal displacement,  $U_\theta$  and  $U_z$ , of the rest of the skin nodes on boundary 3 are connected with the corresponding displacements of the load application node by MPC's. The stiffener nodes are only connected in longitudinal direction  $U_z$ .

The compression and shear load application is force-controlled. With such a load application a constant stress ratio at each load step of a nonlinear analysis is granted.

### 2.3. Verification with analytical solutions

Pflüger [1] describes numerous analytical solutions for the different buckling load types of rectangular plates and shells.

The critical buckling stress of a simply supported rectangular flat plate uniformly compressed in one direction can be calculated by the equation of Timoshenko [2]:

$$(1) \quad \sigma_{cr} = k \cdot \frac{\pi^2 E}{12(1-\nu^2)} \cdot \left(\frac{t}{b}\right)^2$$

with

$$(2) \quad k = \left(\frac{m}{\alpha} + \frac{\alpha}{m}\right)^2$$

$$(3) \quad \alpha = \frac{a}{b}$$

The buckling factor is equal to  $k=4,0$  for the aspect ratio of the skin panel. The factor is equal to  $k=6,97$  for a rectangular flat plate with fixed edges. The real boundary conditions of the stiffened skin panel lie in between, because of the stiffeners, which have a supporting effect. In a linear buckling analysis with ANSYS, a buckling factor of  $k=5,98$  was calculated for the lowest mode shape.

Pflüger [1] gives an analytical solution for cylindrical shell panels due to axial compression. The curvature of the shell  $\omega$  influences the buckling factor.

$$(4) \quad \omega = \frac{b}{\pi} \cdot \frac{\sqrt[4]{12(1-\nu^2)}}{\sqrt{r \cdot t}}$$

The buckling factor for slightly curved shells with  $\omega \leq 2$  is the result of the following equation:

$$(5) \quad k = 4 + \frac{\omega^4}{4}$$

The linear buckling analysis with ANSYS of the curved skin panel stiffened with stringers and frames yields a buckling factor of  $k=6,32$ . This factor contains the supporting effect of the stiffeners and the influence of the shell curvature.

## 3. TRIANGULAR STIFFENED STRUCTURES

The triangular stiffened structures are designed starting from the rectangular stiffened reference structure. These structures shall describe the same section of the fuselage and exhibit the same volume as the reference structure. Every stiffening member of the reference structure is substituted by a tilted stiffener (FIG 3). The results are panels with a triangular skin.

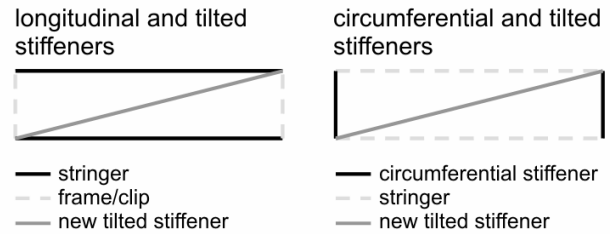


FIG 3. Design concepts for the triangular structures

The geometric correlations of the stiffening members result from the Pythagorean theorem:

$$(6) \quad \ell_{til} = \sqrt{\ell_{str}^2 + \ell_{fr}^2}$$

with  $\ell_{str}$  = stringer spacing and  $\ell_{fr}$  = frame spacing

The volumes of the stiffening members of the reference structures and the triangular structures are:

$$(7) \quad V_{sum} = A_{str} \cdot \ell_{str} + A_{fr} \cdot \ell_{fr}$$

Several assumptions, e.g. using two-dimensional thin shell elements for the three-dimensional fuselage panel, were made in the numerical analysis of the reference structure. These assumptions as well as the boundary conditions are equal in the analysis of the triangular stiffened structures.

The mesh density of the triangular stiffened structure is equal to the mesh density of the reference structure, too. Moreover, the same element type, a 4-node shell element, is used for these structures.

Again, the finite element discretisation must also be quite fine, since the critical mode shapes of a triangular stiffened skin may be more complex than the mode shapes of a rectangular stiffened skin.

### 3.1. Triangular structure with longitudinal and tilted stiffeners

The structure is built up of longitudinal and tilted stiffeners (FIG 4). The frames, clips and stringers of the conventional structure are substituted by new stiffening members. They are designed with T-cross sections for manufacturing reasons.

The cross sectional area  $A_{tri,1}$  of the longitudinal and tilted stiffening members is calculated from:

$$(8) \quad A_{tri,1} = \frac{V_{sum}}{\ell_{str} + \ell_{til}}$$

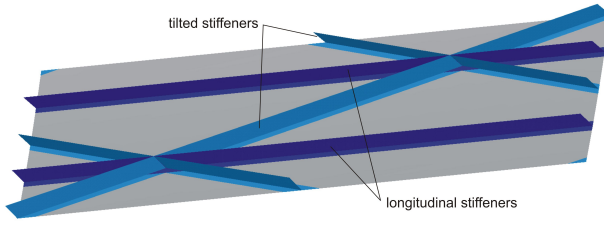


FIG 4. Geometry of the triangular structure with longitudinal and tilted stiffeners

### 3.2. Triangular structure with circumferential and tilted stiffeners

The triangular structure with circumferential and tilted stiffeners is generated in two ways. Both versions have tilted stiffeners which substitute the longitudinal stringers. The cross sectional area of the stringers is converted to the tilted stiffeners:

$$(9) \quad A_{\text{str}} \cdot \ell_{\text{str}} = A_{\text{til},2} \cdot \ell_{\text{til}} \Leftrightarrow A_{\text{til},2} = \frac{A_{\text{str}} \cdot \ell_{\text{str}}}{\ell_{\text{til}}}$$

The design of the circumferential stiffeners is the sole difference. The given frames and clips of the reference structure persist in one version. This version is a partly integral structure because the frames and clips are riveted to the skin.

A complete integrally manufactured structure is analysed for the second triangular structure type. Thus, the second version has integral circumferential stiffeners with a T-cross section and the same cross sectional area as the frame-clip combination. See FIG 5 for the geometry of the two considered types.

The two different stiffener types afford the ability to analyse the influence of the circumferential stiffeners on the buckling behaviour.

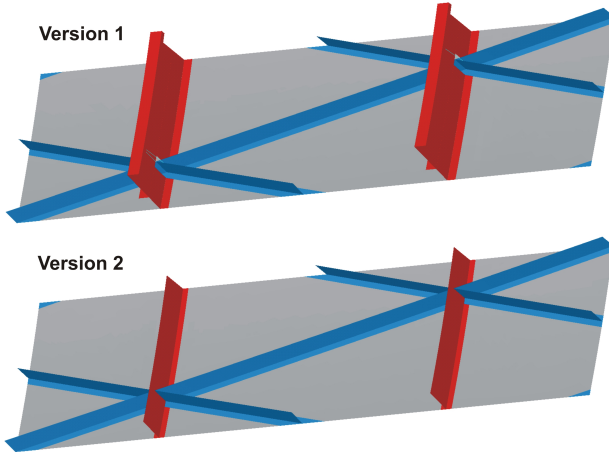


FIG 5. Geometry of the two versions for a triangular structure with circumferential and tilted stiffeners

### 3.3. Analytical solutions for triangular plates

By means of simple finite element models, buckling behaviour due to compression is compared to analytical solutions in the literature. The finite element model of the triangular structure is made of shell elements for the skin and beam elements for the stiffening members.

Amongst other methods Heesch [5] presents approaches

for calculating the buckling factors of right-angled isosceles and equilateral triangular plates uniformly compressed in one direction. These approaches are the basis for the considered structures with isosceles triangular skin panels.

Just like a rectangular stiffened plate the influence of the shell curvature increases the buckling factor.

## 4. MATERIAL MODEL

Plastic material behaviour is included in the finite element panel models of the reference and the triangular structures. Geometrical and plastic nonlinear calculations reflect the real behaviour of the structures.

Published Ramberg-Osgood data have been used as a basis of the finite element input. The Ramberg-Osgood equation (10) combined with an elliptical smoothing curve (HSB [3]) describes the elastic plastic material behaviour (FIG 6).

$$(10) \quad \varepsilon = \frac{\sigma}{E} + 0,002 \left( \frac{\sigma}{R_{p0,2}} \right)^n \quad \text{for } \sigma \leq R_{p0,2}$$

The ellipse is defined by the approach

$$(11) \quad \left( \frac{\varepsilon_{EL}}{\varepsilon_{HA}} \right)^2 + \left( \frac{\sigma_{EL}}{\sigma_{HA}} \right)^2 = 1$$

and runs through point 1 and 2. The gradient in point 1 is equal to  $E_{t1}$ . The ellipse has a horizontal tangent in point 2. Any point of the stress-strain curve is defined by equation (12) and (13).

$$(12) \quad \varepsilon(\sigma) = A - \varepsilon_{HA} \sqrt{1 - \frac{(\sigma - R_m + \sigma_{HA})^2}{\sigma_{HA}^2}}$$

$$(13) \quad \sigma(\varepsilon) = R_m + \sigma_{HA} \left( \sqrt{1 - \frac{(\varepsilon - A)^2}{\varepsilon_{HA}^2}} - 1 \right)$$

A multilinear isotropic hardening using von Mises plasticity is used as a material model in ANSYS. The method expects that the yield surface uniformly expands in all directions. As soon as plastic strains appear, the yield stresses increase in all stress directions.

Stresses and strains of the stress-strain curve are converted into a real stress-strain curve by the following equations [4]:

$$(14) \quad \varepsilon_W = \ln(1 + \varepsilon)$$

$$(15) \quad \sigma_W = \sigma \cdot (1 + \varepsilon)$$

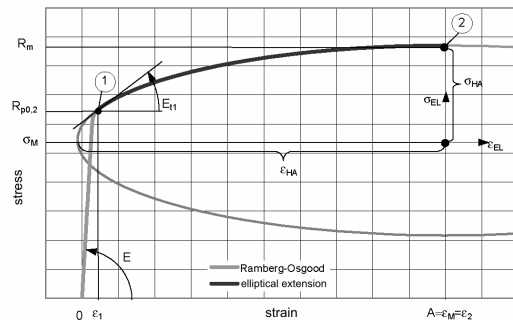


FIG 6. Stress-strain curve [3]

#### 4.1. Used materials

Usual aluminium alloys are used for the riveted reference structure. The skin is made up of aluminium copper alloy 2024 and the stiffeners of aluminium zinc alloy.

These materials are not considered for the integrally stiffened triangular structures. Weldable aluminium magnesium silicon alloys or new aluminium lithium alloys are used. Aluminium lithium alloys offer a lower density, a higher modulus of elasticity and higher tensile strength in comparison to the conventional aluminium copper and aluminium zinc alloys.

### 5. RECTANGULAR STIFFENED INTEGRAL STRUCTURE

The reference structure and the integral triangular structures are made of different aluminium alloys. The modulus of elasticity of the material affects the critical buckling stress (1). A potential advantage of the triangular structures could also be ascribed to improved material properties.

The influence of the different materials can be ruled out with a modified reference structure. A rectangular stiffened integral structure is modelled with the same material properties as the triangular stiffened structures. This structure has longitudinal stringers with a T-cross section.

### 6. BUCKLING ANALYSIS

Two types of buckling analyses are available in ANSYS [6]: a linear elastic stability analysis and a nonlinear stability analysis. The linear elastic stability analysis predicts the theoretical buckling strength of an ideal linear elastic structure. In general, imperfections, geometrical and physical nonlinearities prevent a real structure to reach the theoretical buckling strength. These circumstances can be considered in a nonlinear analysis.

The rectangular and triangular stiffened structures are compared on the basis of the results of both types of analysis (FIG 10).

Critical mode shapes are calculated within the linear elastic stability analysis. The lowest eigenvalue, which have been calculated within this analysis, characterise the critical buckling point of the stiffened structure. Normally the corresponding mode shape shows pure skin buckling, i.e. local buckling, between the stiffening members.

At the beginning of the nonlinear buckling analysis an imperfection is applied to the geometry of the structure. The maximal displacements of the mode shapes, which have been calculated with a linear elastic stability analysis, are scaled from 1/10 to 1/4 of the skin thickness.

Various load combinations of shear and compression are compared with the aid of interaction diagrams. The interaction diagram consists of 10 values: uniform compression, a shear to compression ratio of 0.25, 0.33, 0.5, 0.75, 1.0, 2.0, 3.0, 4.0 and uniform shear. The stress values in the interaction diagrams are normalised with respect to the stress values of pure compression or shear respectively of the reference structure.

#### 6.1. Linear elastic stability analysis

Prior to a linear elastic stability analysis the solver needs a static solution of the problem. The linear elastic stability analysis requires the stress stiffness matrix to be calculated [6]. The eigenvalues, which have been calculated in a linear elastic stability analysis, represent load factors  $\lambda$  for local skin buckling. The critical buckling load is the result of the multiplication of the load factor and the applied compression or the shear force respectively:

$$(16) F_{C,cr} = \lambda \cdot F_C \quad \text{or} \quad F_{S,cr} = \lambda \cdot F_S$$

The critical buckling stress is calculated from these critical buckling loads distributed over the corresponding area.

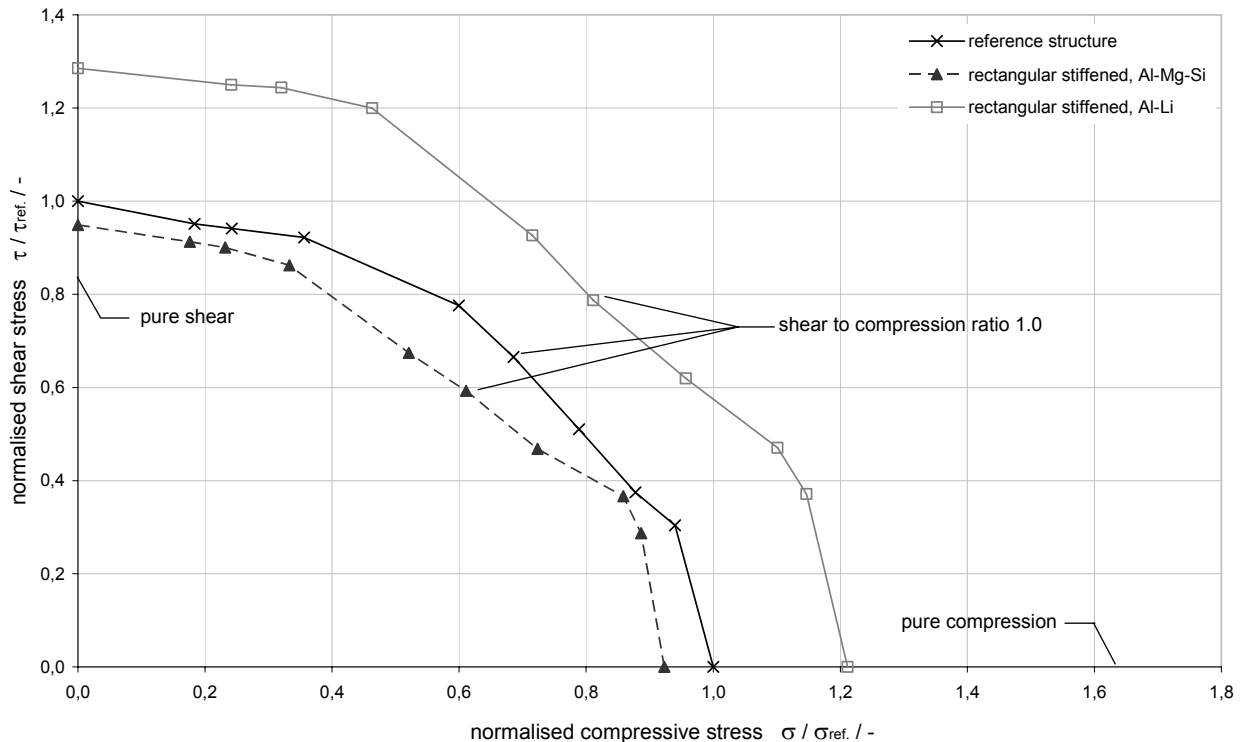


FIG 7. Interaction diagram with the results of nonlinear stability analyses for a rectangular structure made of different materials

The corresponding area for the compression is the complete surface of the skin and the stiffeners on boundary 3 in FIG 2. The shear forces are only applied to the skin and therefore the corresponding area for the shear is the skin surface.

## 6.2. Nonlinear buckling analysis

The load application is force-controlled for the analyses in this paper. This method is chosen because the stress ratio between shear and compression is constant at each load step of the nonlinear buckling analysis.

In a force-controlled analysis the classic Newton-Raphson approach is only able to represent the load vs. deflection curve until the load maximum is reached. The method does not converge if the tangent stiffness is zero.

The arc-length method can solve the nonlinear post-buckling within a force-controlled analysis. The arc-length method varies the arc-length radius according to the involved degree of nonlinearity at each substep during the solution.

The failure criterion for the numerical analysis is defined as the load maximum reached in a load vs. deflection curve. After the load maximum is reached the load bearing capacity decreases while the deflections increase simultaneously.

The several load cases shown in the interaction diagram are calculated with different geometric imperfections. The calculation with the smallest load maximum is taken as the critical failure mode. The analysis requires many calculations with different imperfections, because the most disadvantageous imperfection cannot be predicted beforehand.

## 6.3. Influence of the material on the buckling behaviour

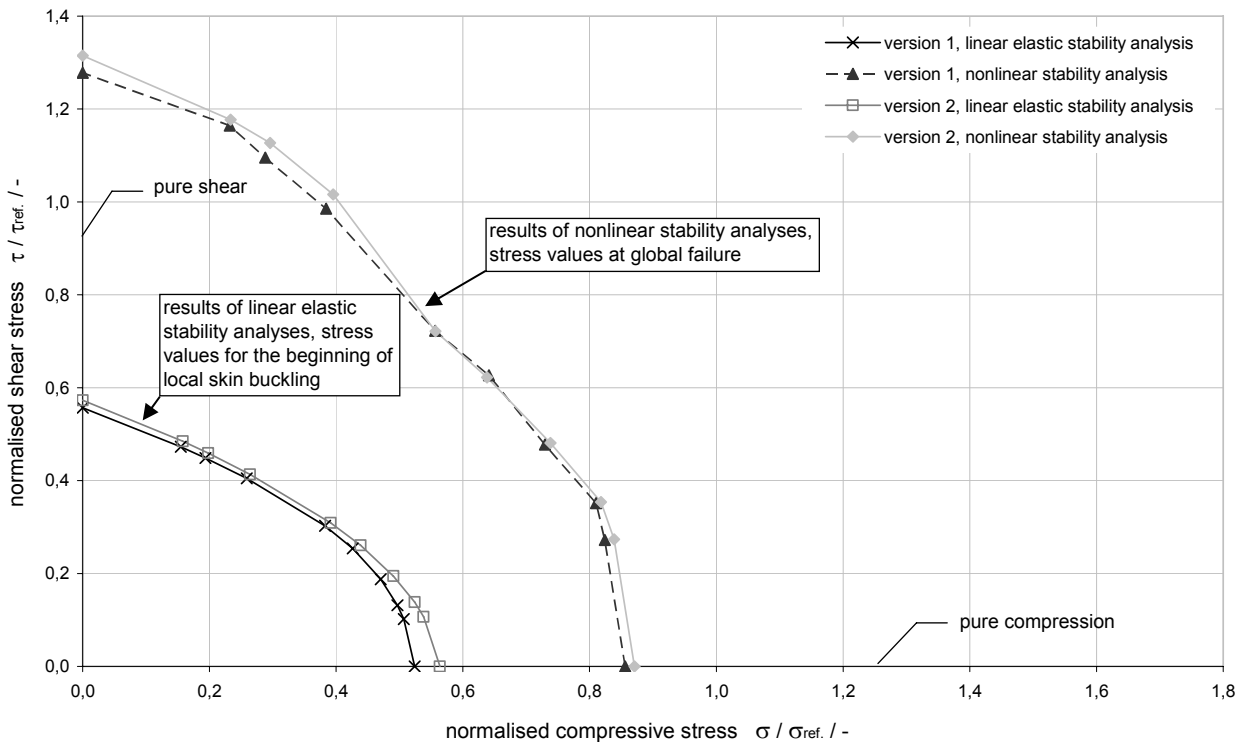


FIG 8. Interaction diagrams for the triangular structures with circumferential and tilted stiffeners

FIG 7 describes the influence of the different materials on the nonlinear buckling behaviour of a rectangular stiffened structure. The figure shows an interaction curve for the reference structure. The skin is made up of 2024 alloy. It is stiffened by stringers with a L-cross section and a frame clip combination made up of aluminium zinc alloys. The two other curves characterise the nonlinear buckling behaviour of the rectangular stiffened integral structure with T-cross sectional stringers. The shapes of these two curves are similar. When compared to the curve of the reference structure the curves show differences in the range of  $\tau/\sigma=0.25$  to 2.0. These different shapes can be ascribed to the different cross sections of the longitudinal stringers. The material influences the level of the compressive and shear stresses merely.

The interaction diagrams of the various triangular structures show the same characteristics. Materials with a higher tensile strength, e.g. aluminium lithium alloys, exhibit higher compressive and shear stresses.

The following investigations concentrate on structures made up of aluminium lithium to analyse the influence of the geometry. They also apply to other materials like aluminium magnesium silicon alloys.

## 6.4. Influence of circumferential stiffeners on the buckling behaviour

The influence is analysed within a linear elastic stability analysis and a nonlinear stability analysis of the two versions of the triangular structure stiffened with circumferential and tilted elements. FIG 8 shows the interaction diagram for the structures with different types of circumferential stiffeners. Each structure is represented with a curve for the linear elastic and the nonlinear solution.

The curves of the two types of analysis for compressive and shear stress differ by a few per cent. In both cases version 2 of the triangular structure with circumferential and tilted stiffeners (FIG 5) exhibits higher stresses. The

reason for the stress differences between the two versions are the different geometries of the circumferential stiffeners, particularly the geometry of the stiffener flanges. The T-cross sections of version 2 have a wider flange than the clips of version 1. The wider flange of version 2 reduces the free unstiffened skin surface and decreases the aspect ratio. This leads to an increase of the buckling factor  $k$  and the critical buckling stress  $\sigma_{cr}$  or  $\tau_{cr}$  accordingly. These correlations are shown in equations (1) to (3). The minimal larger free unstiffened skin panel of version 1 exhibits lower critical buckling stresses than the skin panel of version 2.

The structure with the T-cross sectional circumferential stiffener is used for the following comparisons between rectangular and non-rectangular stiffened structures.

## 6.5. Comparison between the buckling behaviour of rectangular and non-rectangular stiffened structures

FIG 10 shows the interaction diagrams for the various stiffening types, calculated by a linear elastic stability analysis and a nonlinear stability analysis. The values of the curves for linear elastic stability analyses represent the stresses at the beginning of local skin buckling. The values of the curves for nonlinear stability analysis are stresses of the global failure of the structure. The results of these two types of analysis are quite different and now described further.

### 6.5.1. Linear elastic stability analysis

The triangular structure with circumferential and tilted stiffeners shows significantly lower stresses than the rectangular structure. The stress values are up to 50 % lower. In contrast to that, the triangular structure with longitudinal and tilted stiffeners provides up to 50 % higher

stress values. The buckling of this structure occurs at higher stresses than the buckling of the triangular structure with circumferential and tilted stiffeners.

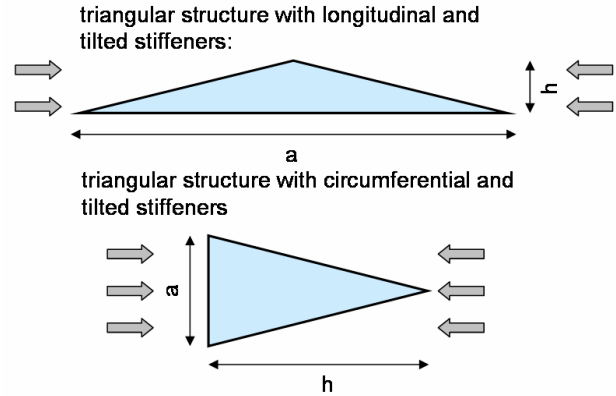


FIG 9. Skin panels of the triangular structures uniformly compressed in one direction

Pflüger [1] describes the influence of the aspect ratio  $h/a$  on the buckling factor  $k$  and the critical buckling load. A higher aspect ratio  $h/a$  causes a higher buckling factor (FIG 9). But the height of the triangle is quadratic in the denominator of the formula for the critical buckling load. The critical buckling stress decreases with an increasing height of the triangle.

### 6.5.2. Nonlinear buckling analysis

The interaction curves of the nonlinear buckling analysis show different trends. Above values of  $\tau/\sigma \approx 2.0$  the stresses of the triangular structure with circumferential and tilted stiffeners are higher than the stresses of the other triangular structure.

The triangular structures show higher stresses in comparison with the rectangular stiffened structure at

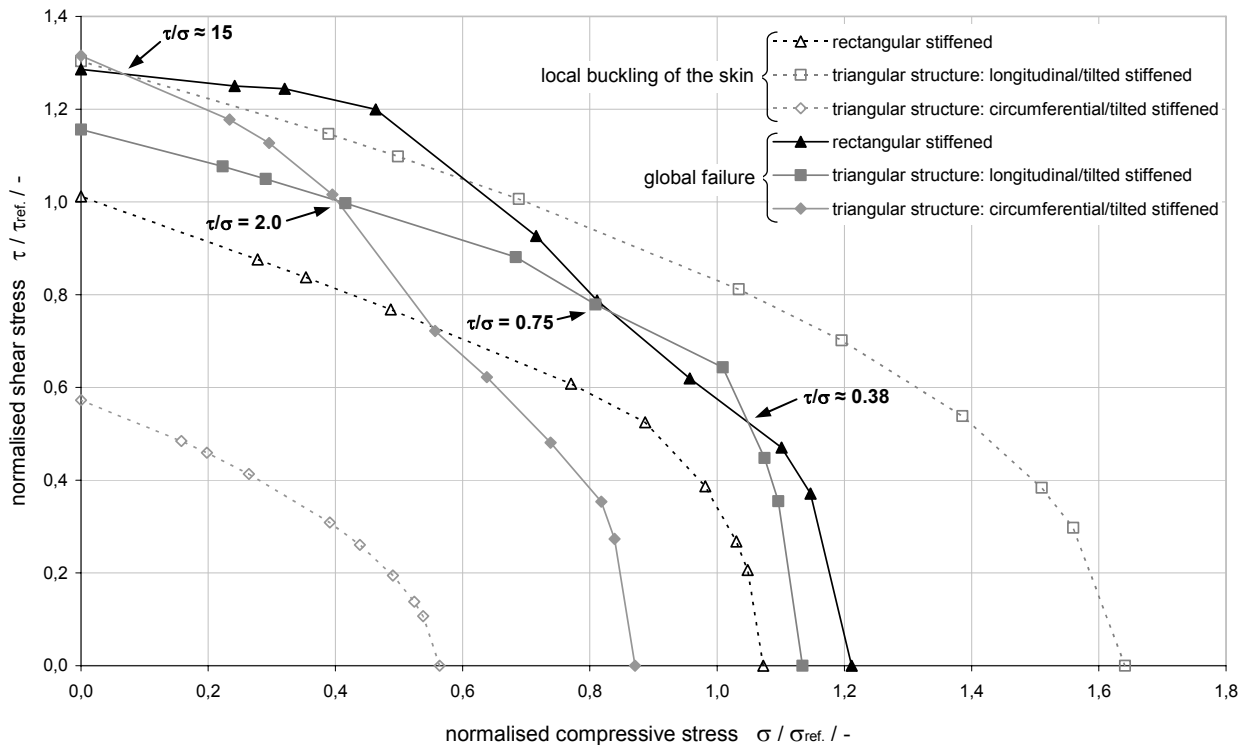


FIG 10. Interaction diagrams for local skin buckling and global failure for the rectangular and triangular stiffened structures

some points of the interaction diagram. The triangular structure with longitudinal and tilted stiffeners provides advantages within the range of  $\tau/\sigma \approx 0.38$  to 0.75. The triangular structure stiffened by circumferential and tilted stiffeners has slight advantages over the reference structure in regions with high values of  $\tau/\sigma \approx 15$  or pure shear stress.

## 7. CONCLUSION AND PERSPECTIVE

The analyses showed that in some ranges of compressive and shear stresses, the buckling behaviour of the different triangular structures have advantages over the conventional rectangular stiffened fuselage structures. The focus of the described analyses was to design structures with the same weight as the reference structure. In the next steps, triangular stiffened structures with the same properties like the reference structure will be investigated because they provide the capability to reduce the weight of the fuselage.

Triangular structures with circumferential and tilted stiffeners can be applied to regions with principal shear stresses, like the side shell of a fuselage.

Triangular structures with longitudinal and tilted stiffeners can be applied in regions with higher compressive stresses. But the lack of circumferential stiffeners can cause other problems like a decreasing capability of a fuselage to keep its cylindrical cross section.

These investigations concentrated on buckling analyses. Usually stiffened structures are also used to cope with damage tolerance problems. Integrally stiffened structures may have some problems with respect to this regard. Therefore, further investigations will have to be carried out prior to real applications.

## REFERENCES

- [1] Pflüger, A., *“Stabilitätsprobleme der Elastostatik“*, Springer, 3<sup>rd</sup> edition 1975
- [2] Timoshenko, S. and Gere, J., *“Theory of elastic stability“*, McGraw-Hill, 2<sup>nd</sup> edition 1961
- [3] HSB, Handbuch Strukturberechnung, 2000
- [4] Rösler, J., Harders, H. and Bäker, M., *“Mechanisches Verhalten der Werkstoffe“*, Teubner, 2003
- [5] Heesch, O., *“Die Berechnung der Beulspannungen ebener Platten mit Hilfe von Differenzengleichungen unter besonderer Berücksichtigung von Dreiecksplatten“*, Dissertation Hannover, 1936
- [6] Release 10.0 Documentation for ANSYS, ANSYS Inc., Canonsburg, USA
- [7] Heitmann, M., *“Untersuchung des Nachbeulverhaltens rechteckig versteifter metallischer Strukturen unter kombinierter Druck- und Schubbeanspruchung“*, Dissertation Braunschweig, 2005